

This article was downloaded by: [University of California, San Diego]

On: 07 August 2012, At: 12:13

Publisher: Taylor & Francis

Informa Ltd Registered in England and Wales Registered Number: 1072954 Registered office: Mortimer House, 37-41 Mortimer Street, London W1T 3JH, UK



## Molecular Crystals and Liquid Crystals

Publication details, including instructions for authors and subscription information:

<http://www.tandfonline.com/loi/gmcl20>

### Preparations of Titanium Composite Electrodes from Commercial Inorganic Pigment and Its Application to Light Scattering Layers on Dye-Sensitized Solar Cells

Doo-Wha Kim<sup>a</sup>, Jung-Hyon Kim<sup>a</sup>, Ki-Hyun Kim<sup>a</sup>, Sang-Eun Cho<sup>a</sup>, Won-Pill Hwang<sup>a</sup>, Min-Hye Seo<sup>a</sup>, Mi-Ra Kim<sup>a</sup> & Jin-Kook Lee<sup>a</sup>

<sup>a</sup> Department of Polymer Science & Engineering, Pusan National University, Busan, Korea

Version of record first published: 16 May 2011

To cite this article: Doo-Wha Kim, Jung-Hyon Kim, Ki-Hyun Kim, Sang-Eun Cho, Won-Pill Hwang, Min-Hye Seo, Mi-Ra Kim & Jin-Kook Lee (2011): Preparations of Titanium Composite Electrodes from Commercial Inorganic Pigment and Its Application to Light Scattering Layers on Dye-Sensitized Solar Cells, *Molecular Crystals and Liquid Crystals*, 539:1, 156/[496]-165/[505]

To link to this article: <http://dx.doi.org/10.1080/15421406.2011.566113>

PLEASE SCROLL DOWN FOR ARTICLE

Full terms and conditions of use: <http://www.tandfonline.com/page/terms-and-conditions>

This article may be used for research, teaching, and private study purposes. Any substantial or systematic reproduction, redistribution, reselling, loan, sub-licensing, systematic supply, or distribution in any form to anyone is expressly forbidden.

The publisher does not give any warranty express or implied or make any representation that the contents will be complete or accurate or up to date. The accuracy of any instructions, formulae, and drug doses should be independently verified with primary sources. The publisher shall not be liable for any loss, actions, claims, proceedings, demand, or costs or damages whatsoever or howsoever caused arising directly or indirectly in connection with or arising out of the use of this material.

# Preparations of Titanium Composite Electrodes from Commercial Inorganic Pigment and Its Application to Light Scattering Layers on Dye-Sensitized Solar Cells

DOO-WHA KIM, JUNG-HYON KIM, KI-HYUN KIM,  
SANG-EUN CHO, WON-PILL HWANG,  
MIN-HYE SEO, MI-RA KIM, AND JIN-KOOK LEE

Department of Polymer Science & Engineering, Pusan National University, Busan, Korea

*We synthesized three  $\text{TiO}_2$  composite ( $\text{TiO}_2\text{-Al}_2\text{O}_3$ ,  $\text{TiO}_2\text{-Nb}_2\text{O}_5$ , and  $\text{TiO}_2\text{-ZrO}_2$ ) electrodes by the hydrothermal method using titanium dioxide pigment and fabricated double layer dye-sensitized solar cells (DSSCs) using the  $\text{TiO}_2$  composites as the scattering layer. Due to their enhanced light harvesting capability, the performance of the double layer DSSCs with  $\text{TiO}_2$  composite top layer was better than that of the cells without the  $\text{TiO}_2$  composite top layer. A maximum power conversion efficiency of 6.68% was obtained for the double layer DSSCs with  $\text{TiO}_2\text{-Al}_2\text{O}_3$  composite layer under AM 1.5 illumination.*

**Keywords** Dye-sensitized solar cells; light scattering effect; titanium dioxide composite electrodes

## 1. Introduction

Dye-Sensitized Solar Cells (DSSCs) have been extensively studied as an environmentally-friendly energy source. Their main advantages are a high energy conversion efficiency, simple production process, and low manufacturing cost [1–3]. Recently, many researchers have focused on finding new dyes to improve the light-harvesting ability of DSSCs by developing new electron-transfer mediators to replace the volatile and corrosive iodide/triiodide redox system and studying the size and shape of the semiconductor electrodes to determine their influence on the photoelectric performance of DSSCs [4–7].

The photovoltaic effect in DSSCs occurs at the interface between the dye-anchored wide band-gap oxide semiconductor and the electrolyte. The charge separation at the dye-photoelectrode interface is energetically and entropically

---

Address correspondence to Mi-Ra Kim or Jin-Kook Lee, Department of Polymer Science & Engineering, Pusan National University, Busan, 609-735, Korea. Tel.: +82-51-510-2405; Fax: +82-51-513-7720; E-mail: mrkim2@pusan.ac.kr; leejk@pusan.ac.kr

avored, because the conduction band of the metal oxide is at a lower energy than the LUMO of the dye and the electronic energy states in the conduction band of the semiconductor have a larger density than the molecular orbital of the dye [8]. Many kinds of wide band-gap oxide have been tested for use as the photoelectrodes in DSSCs [9–16]. Among them,  $\text{TiO}_2$  is relatively cheap and abundant. However, most titanium dioxide pigments used in the paints and plastic industry have a large particle size for the sake of their whiteness and opacity. Therefore, photoelectrodes consisting of titanium dioxide pigments do not show good performance in DSSCs. In order to use titanium dioxide pigments as the photoelectrode in DSSCs, in the present research, titanium dioxide pastes were made using reformed titanium dioxide pigment. The key factor determining the performance of the photoelectrodes in DSSCs is the particle size and distribution of the metal oxide. Their performance can be improved by using titanium dioxide with a larger surface area [1].

In order to improve the conversion efficiency and suppress the recombination processes, composite electrodes [17,18] and electrodes with a core/shell structure [19–21] have been used in DSSCs. In this study, three  $\text{TiO}_2$  composite electrodes were made by the hydrothermal method using titanium dioxide pigment. They were characterized by BET specific surface area measurements, X-ray diffraction, and X-ray fluorescence. Also, the light scattering effect and performance of the DSSCs using the  $\text{TiO}_2$  composite electrodes were confirmed by their UV-Vis-NIR data and I-V curves, respectively.

## 2. Experimental

### 2.1. Materials

$\text{ZrO}_2$  was made using zirconium chloride (Kanto chem. Co. Inc) which was hydrolyzed by water and calcined at  $500^\circ\text{C}$ . KA100  $\text{TiO}_2$  (Cosmo chemical. co., Ltd., Korea),  $\text{Al}_2\text{O}_3$ , and  $\text{Nb}_2\text{O}_5$  (Aldrich) were used as received. Titanium(IV) isopropoxide, iodine ( $\text{I}_2$ ), and tetrabutyl ammonium iodide (TBAI) were purchased from Aldrich. Tetrametylammonium hydroxide solution (25%) was purchased from Acros. N719 dye, viz. *cis*-bis(isothiocyanato)bis(2,2'-bipyridyl-4,4'-dicarboxylato) ruthenium(II) (Solchem. Co., Ltd., Korea), was used as the sensitizer. 1-Propyl-3-methylimidazolium iodide (PMII) as an ionic liquid and HT/SP  $\text{TiO}_2$  paste (particle size: 9 nm) were purchased from Solaronix SA. Fluorine-doped tin oxide,  $\text{SnO}_2:\text{F}$  glass (Asahi,  $15\ \Omega$ , 2.2 T) was used as a transparent conductive electrode.

### 2.2. Synthesis of Reformed $\text{TiO}_2$ Composites

The  $\text{TiO}_2$  pigment, which is used in the paints and plastic industry, was reformed by the hydrothermal method. 4 g of titanium(IV) isopropoxide was added to 100 mL of methanol. Under vigorous stirring, 8 g of KA100  $\text{TiO}_2$  powder and 1 g of  $\text{Al}_2\text{O}_3$  powder were added to the prepared methanol solution and then 100 mL of 0.1 M nitric acid solution at pH 1 was added dropwise to the  $\text{TiO}_2$ - $\text{Al}_2\text{O}_3$  composite slurry under strong stirring, and the stirring was continued for an additional 1 h after all of the drops were added. The resultant colloidal solution was transferred to a closed autoclave and subjected to hydrothermal synthesis for 12 h at  $260^\circ\text{C}$ . After the hydrothermal synthesis, the  $\text{TiO}_2$ - $\text{Al}_2\text{O}_3$  composite was separated by filtration with filter paper

and sufficiently washed with ion-exchanged water. The final product was dried at 80°C for 24 h, yielding a white powder. The  $\text{TiO}_2\text{-Nb}_2\text{O}_5$  composite and the  $\text{TiO}_2\text{-ZrO}_2$  composite were obtained in the same manner except for the kind of minor oxide that was used.

### 2.3. Preparations of Reformed $\text{TiO}_2$ Composite Pastes

Three types of reformed  $\text{TiO}_2$  composite pastes were prepared by the process shown in Figure 1. The mixed  $\text{TiO}_2$  powders were composed of KA100  $\text{TiO}_2$  with  $\text{Al}_2\text{O}_3$ ,  $\text{Nb}_2\text{O}_5$  or  $\text{ZrO}_2$ , at a weight ratio of 9:1. Paste A was fabricated from only KA100  $\text{TiO}_2$  powder, Paste B was the  $\text{TiO}_2\text{-Al}_2\text{O}_3$  composite, Paste C was the  $\text{TiO}_2\text{-Nb}_2\text{O}_5$  composite, and Paste D was the  $\text{TiO}_2\text{-ZrO}_2$  composite.

### 2.4. Fabrication of DSSC Devices Using Reformed $\text{TiO}_2$ Composites

As shown in Figure 2, four single type and three double type electrodes were deposited onto  $\text{SnO}_2\text{:F}$  glass by the doctor-blade method and subsequent calcination process at 500°C. The dye (N719) covered  $\text{TiO}_2$  electrode and Pt-counter electrode were assembled into a sandwich type cell. The space between the electrodes was filled with the electrolyte (0.1 M LiI, 0.05 M  $\text{I}_2$ , 0.6 M 1-propyl-3-methylimidazolium iodide, 0.5 M *tert*-butylpyridin in acetonitrile) by capillary force. Finally, the hole was sealed using a hot-melt film and cover glass.

### 2.5. Measurements

The thickness of the  $\text{TiO}_2$  electrodes was found to be about 4~20  $\mu\text{m}$  by SEM measurements (S-4200 HITACHI). The diameter of the particles was estimated from the TEM (JEOL JEM-2010) images. X-ray diffraction with Cu  $\text{K}\alpha$  radiation (X'Pert

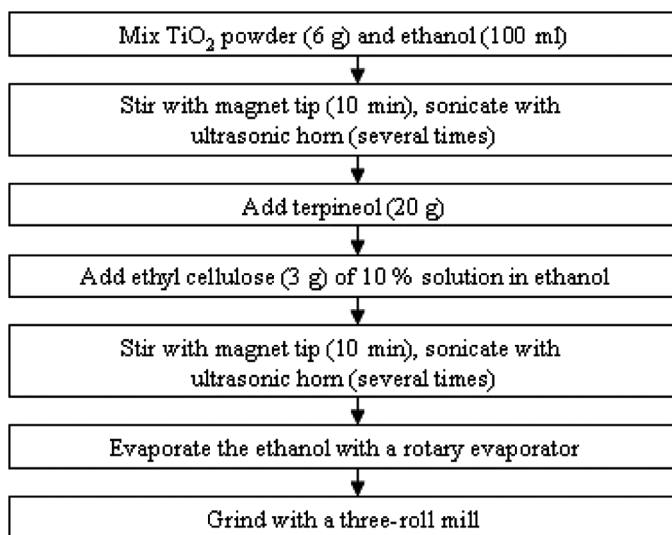


**Figure 1.** Fabrication process of  $\text{TiO}_2$  composite pastes for DSSCs.

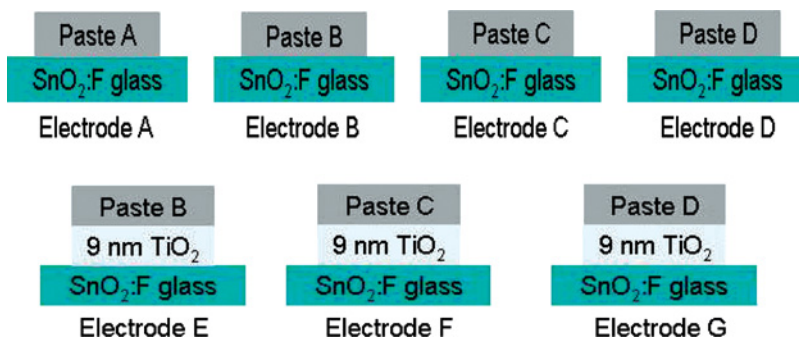


**Figure 2.** Four single layer (upper) and three double layer (down) of  $\text{TiO}_2$  composite electrodes onto  $\text{SnO}_2\text{:F}$  glass for DSSCs.

PRO) showed that the  $\text{TiO}_2$  composites mainly consisted of anatase  $\text{TiO}_2$  and the results of the X-ray fluorescence (SEA1200VX ID\_1147) measurements confirmed the existence of the various composite oxides. The Brunauer-Emmett-Teller (BET) surface area and pore volume and mean pore size of the  $\text{TiO}_2$  composite powder were determined by a Surface Area & Pore Size Analyzer (NOVA 4000e). The transmittance and absorbance of the  $\text{TiO}_2$  composite electrodes were measured using a UV-Vis-NIR spectrophotometer (Varian, Cary 5000). The photovoltaic characteristics of the DSSCs were measured using a Solar Simulator (150 W simulator, PEC-L11/PECCELL) under simulated solar light with an ARC Lamp power supply (AM 1.5,  $100 \text{ mW}/\text{cm}^2$ ). The solar simulator was calibrated to a verified Si reference cell. The active area of the DSSC was adjusted to  $0.25 \text{ cm}^2$ .

### 3. Results and Discussion

#### 3.1. Characterizations of Reformed $\text{TiO}_2$ Composite Electrodes

Figure 3 shows the X-ray diffraction-patterns of the films using the KA100  $\text{TiO}_2$  and  $\text{TiO}_2$  composites with  $\text{Al}_2\text{O}_3$ ,  $\text{Nb}_2\text{O}_5$ , and  $\text{ZrO}_2$ . The crystal structures of the particles consisted of both anatase [22] and hongquiiite phases [23] except for Paste A. Pure anatase phase is observed in Figure 3(a). The anatase and rutile crystalline structures of  $\text{TiO}_2$  play an important role in the photovoltaic effects of the DSSCs, but not the hongquiiite crystalline structure. In Figure 3, although the  $\text{TiO}_2$  composites were mixed with different kinds of minor oxides, they had similar XRD-patterns.

Therefore, to obtain more precise results, XRF measurements were performed for the three  $\text{TiO}_2$  composite powders. Each added 1 g of minor oxide appeared by atom ratio and had different weight percentage. Because the XRF data was qualitative and the atom weight of Al is lower than that of Nb or Zr. The XRF data are listed in Table 1.

In addition, we measured the surface area, pore volume, and pore diameter of the  $\text{TiO}_2$  composites by the BET. As shown in Table 2, the surface area of the  $\text{TiO}_2$  composite based on the KA 100  $\text{TiO}_2$  powder was very low ( $14.30 \text{ m}^2/\text{g}$ ), however, the  $\text{TiO}_2$  composites had higher surface areas ( $30\sim 40 \text{ m}^2/\text{g}$ ). Each  $\text{TiO}_2$  composite was composed of the major oxide or  $\text{TiO}_2$  part and the minor oxide part.

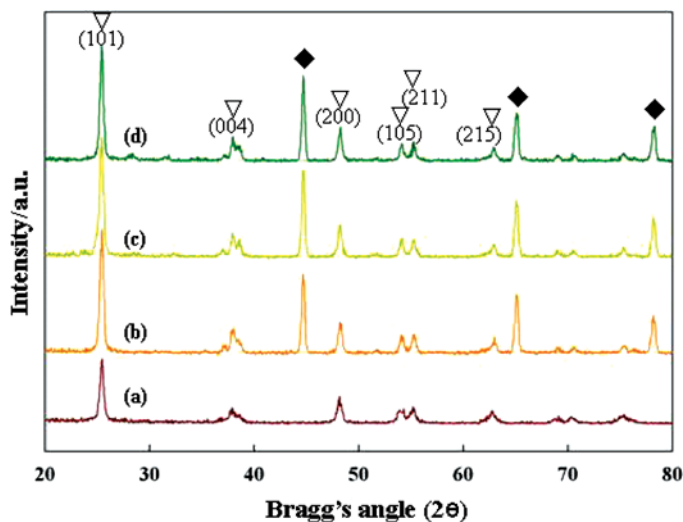


**Figure 3.** The X-ray diffraction-patterns of the  $\text{TiO}_2$  composites calcined at  $500^\circ\text{C}$  [(a) Paste A, (b) Paste B, (c) Paste C, and (d) Paste D].  $\nabla$ , anatase;  $\blacklozenge$ , hongquittite.

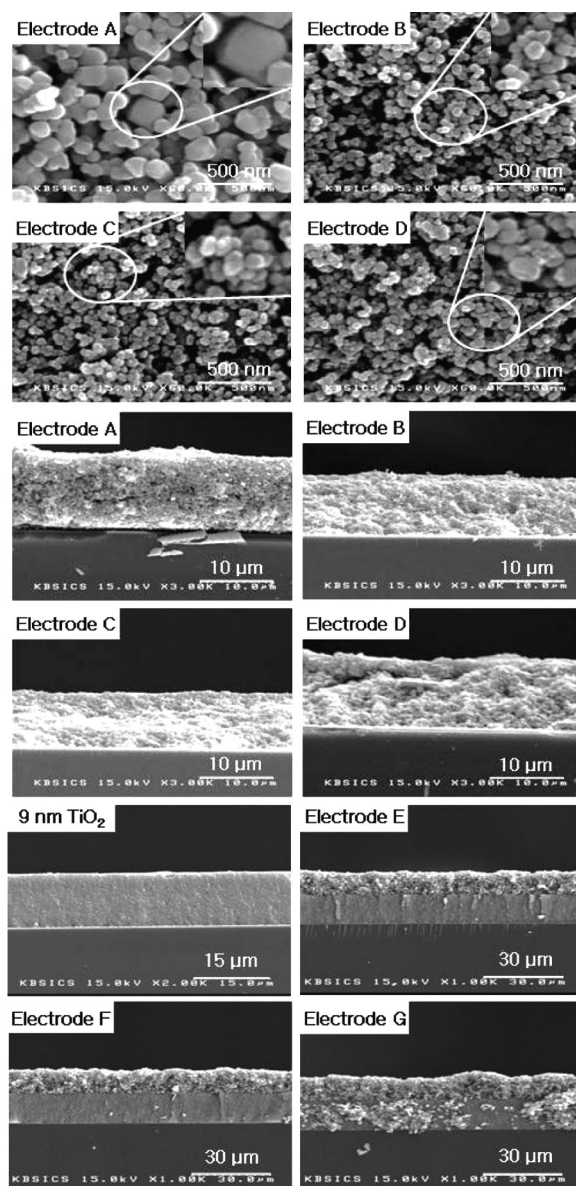
Figure 4 shows the SEM images of the single layer and double layer electrodes on the  $\text{SnO}_2\text{:F}$  glass substrate. The grain sizes of KA100  $\text{TiO}_2$  are between 100 nm and 300 nm and the  $\text{TiO}_2$  composites have an average grain size of 50~100 nm. The thicknesses of the single layer  $\text{TiO}_2$  composites electrodes (Electrode A~D) were

**Table 1.** The XRF data of  $\text{TiO}_2$  composites

	Atom	wt %	Cps	Filter	Condition
$\text{TiO}_2\text{-Al}_2\text{O}_3$ composite	Ti	88.34 ( $\pm 0.34$ )	9761.233 ( $\pm 38.211$ )	used Cr	Vacuum
	Al	11.66 ( $\pm 1.49$ )	55.062 ( $\pm 7.141$ )	used Cl	Vacuum
$\text{TiO}_2\text{-Nb}_2\text{O}_5$ composite	Ti	97.98 ( $\pm 0.27$ )	12603.232 ( $\pm 35.657$ )	used Cr	Air
	Nb	2.02 ( $\pm 0.03$ )	242.171 ( $\pm 3.906$ )	used Cd	Air
$\text{TiO}_2\text{-ZrO}_2$ composite	Ti	95.72 ( $\pm 0.36$ )	9799.244 ( $\pm 38.258$ )	used Cr	Air
	Zr	4.28 ( $\pm 0.05$ )	404.956 ( $\pm 4.714$ )	used Cd	Air

**Table 2.** The BET and Pore data of  $\text{TiO}_2$  composites

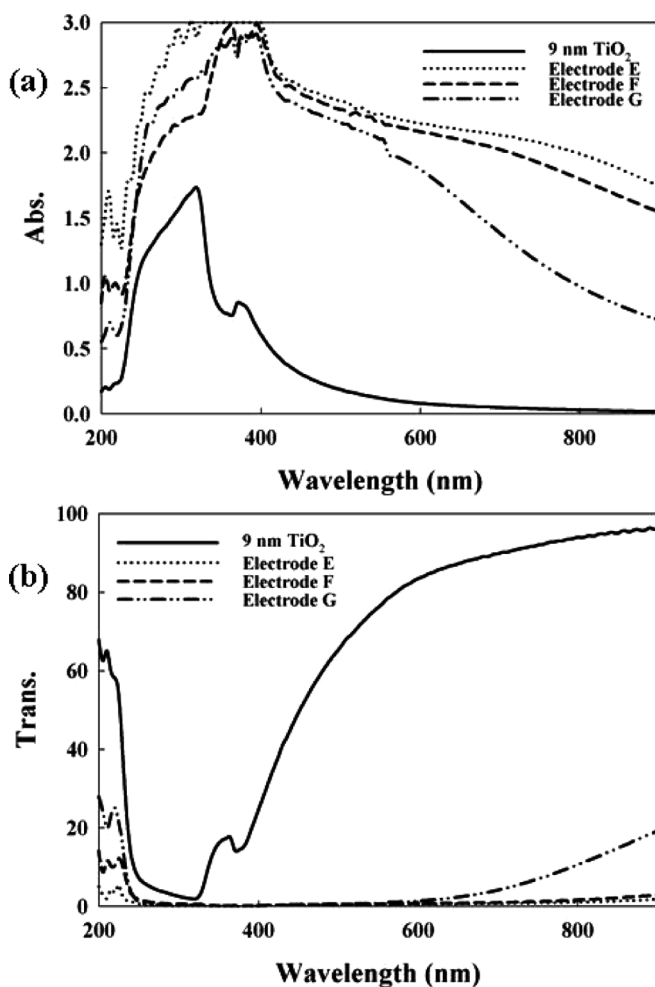
	BET surface area ( $\text{m}^2/\text{g}$ )	Pore volume ( $\text{cm}^3/\text{g}$ )	Pore diameter (nm)
KA-100 $\text{TiO}_2$	14.30	0.1318	7.220
$\text{TiO}_2\text{-Al}_2\text{O}_3$ comp.	32.65	0.1520	6.005
$\text{TiO}_2\text{-Nb}_2\text{O}_5$ comp.	31.07	0.1474	6.058
$\text{TiO}_2\text{-ZrO}_2$ comp.	40.62	0.1825	5.653



**Figure 4.** SEM images of single layer  $\text{TiO}_2$  composite electrodes (A, B, C, and D) and double layer  $\text{TiO}_2$  composite electrodes (9 nm  $\text{TiO}_2$ , E, F, and G) on the  $\text{SnO}_2:\text{F}$  glass after sintering at  $500^\circ\text{C}$ .

about  $10\sim 12\mu\text{m}$  and those of the double layer  $\text{TiO}_2$  composites electrodes were about  $20\mu\text{m}$  (Electrode E~G).

The UV-Vis absorbance and transmittance spectra of the  $\text{TiO}_2$  composite electrodes are shown in Figure 5. The absorbance values of the double layer  $\text{TiO}_2$  composite electrodes were much higher than those of the single layer electrode. The high absorbance of the  $\text{TiO}_2\text{-Al}_2\text{O}_3$  composite electrode in the region over  $600\text{nm}$  was to be expected, because of its larger grain size. Particularly, in



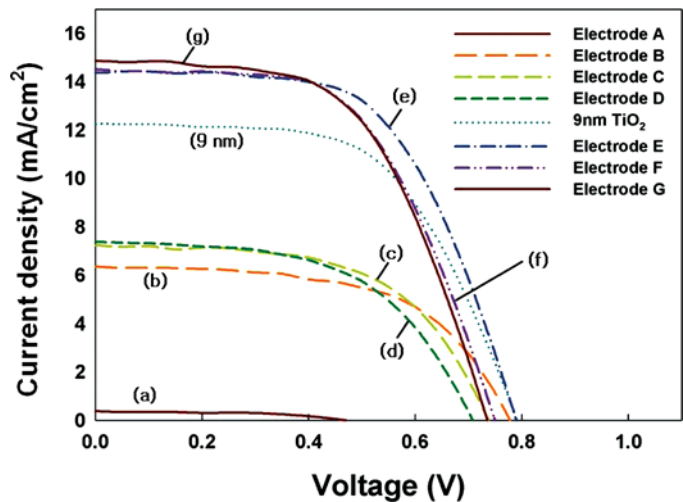
**Figure 5.** Absorbance (a) and transmittance (b) spectra of various  $\text{TiO}_2$  composite electrodes (9 nm  $\text{TiO}_2$ , Electrode E, F, and G) calcined at  $500^\circ\text{C}$  on the  $\text{SnO}_2\text{:F}$  glass.

Figure 5(b), electrodes E and F comprising  $\text{TiO}_2\text{-Al}_2\text{O}_3$  and  $\text{TiO}_2\text{-Nb}_2\text{O}_5$  composite layers, respectively, showed a transmittance of nearly 0% in the visible and near-IR region. In all representations, the light scattering layers comprising larger  $\text{TiO}_2$  particles, such as those with a diameter of 50~100 nm, appear to be promising candidates for light collection.

### 3.2. Photovoltaic Properties of DSSCs using Reformed $\text{TiO}_2$ Composite Electrodes

The photocurrent-voltage characteristics of the DSSCs based on the various  $\text{TiO}_2$  composite electrodes (Electrodes A, B, C, D, E, F, and G) after sintering at  $500^\circ\text{C}$  are presented in Figure 6, and their photovoltaic characteristics are summarized in Table 3. The efficiencies of the DSSCs using the  $\text{TiO}_2$  composite electrodes were much higher than that of the KA-100  $\text{TiO}_2$  electrode (0.09%). This was attributed





**Figure 6.** I-V curves of DSSCs using various TiO<sub>2</sub> composite electrodes under light density: 100 mW/cm<sup>2</sup>; AM 1.5, active area: 0.25 cm<sup>2</sup>.

to the increase of the surface area of the TiO<sub>2</sub> composites after they were reformed by the hydrothermal method (Table 1). Therefore, it was found that the TiO<sub>2</sub> composites reformed by the hydrothermal method have the potential to be activated by a commercial TiO<sub>2</sub> pigment.

Moreover, we fabricated double layer DSSCs using the TiO<sub>2</sub> composites as the scattering layer. Due to their enhanced light harvesting capability, the performance of the double layer DSSCs with the TiO<sub>2</sub> composite top layer is better than that of the DSSCs without the TiO<sub>2</sub> composite top layer. Maximum power conversion efficiencies of 6.18~6.68% were obtained for the double layer DSSCs with TiO<sub>2</sub> composite layers under AM 1.5 illumination. Especially, the highest efficiency was observed for the DSSC with the TiO<sub>2</sub>-Al<sub>2</sub>O<sub>3</sub> composite top layer. This may be because the conduction band edge of Al<sub>2</sub>O<sub>3</sub> is significantly more negative (Al<sub>2</sub>O<sub>3</sub>: -4.45) than those of the other minor oxides (ZrO<sub>2</sub>: -1.24 and Nb<sub>2</sub>O<sub>5</sub>: -0.7) [19].

**Table 3.** Photovoltaic performances of DSSCs under light density: 100 mW/cm<sup>2</sup>; AM 1.5, active area: 0.25 cm<sup>2</sup> using single and double layer TiO<sub>2</sub> composite electrodes

Type of electrode	V <sub>oc</sub> (V)	J <sub>sc</sub> (mA/cm <sup>2</sup> )	Fill Factor	Efficiency (%)
A	0.47	0.38	0.51	0.09
B	0.78	6.35	0.58	2.86
C	0.74	7.23	0.57	3.04
D	0.71	7.37	0.55	2.88
E	0.79	14.4	0.59	6.68
F	0.75	14.5	0.57	6.21
G	0.74	14.9	0.57	6.18
9 nm	0.79	12.3	0.58	5.64

This indicates that the  $\text{TiO}_2\text{-Al}_2\text{O}_3$  composite as a semiconductor has a physically more negative conduction band edge than the other composites.

#### 4. Conclusion

We successfully synthesized three  $\text{TiO}_2$  composite ( $\text{TiO}_2\text{-Al}_2\text{O}_3$ ,  $\text{TiO}_2\text{-Nb}_2\text{O}_5$ , and  $\text{TiO}_2\text{-ZrO}_2$ ) electrodes by the hydrothermal method using titanium dioxide pigment. The efficiencies of the DSSC devices using these  $\text{TiO}_2$  composite electrodes were improved by the enhanced surface area of the reformed  $\text{TiO}_2$  composites. Double layer DSSCs were also fabricated by using the  $\text{TiO}_2$  composites as the scattering layer and their photovoltaic properties were investigated. With the addition of the scattering layers to the double layer  $\text{TiO}_2$  composite electrodes, the photocurrents of the DSSCs were increased by more than 10%, compared to the device using the single layer  $\text{TiO}_2$  electrode without the scattering layers.

#### Acknowledgment

This research was supported by the Converging Research Center Program through the National Research Foundation of Korea (NRF) funded by the Ministry of Education, Science and Technology (20090082141).

#### References

- [1] O'regen, B., & Grätzel, M. (1991). *Nature*, 353, 737.
- [2] Nazeeruddin, M. K., Kay, A., Rodicio, I., Humphry-Baker, R., Muller, E., Liska, P., Valchopoulos, N., & Grätzel, M. (1993). *J. Am. Chem. Soc.*, 115, 6382.
- [3] McConnell, R. D. (2002). *Renewable Sustainable Energy Rev.*, 6, 273.
- [4] Katoh, R., Kasuya, M., Kodate, S., Furube, A., Fuke, N., & Koide, N. (2009). *J. Phys. Chem. C*, 113, 20738.
- [5] Zhang, Z., Chen, P., Murakami, T. N., Zakeeruddin, S. M., & Grätzel, M. (2008). *Adv. Funct. Mater.*, 18, 341.
- [6] Murakoshi, K., Kogure, R., Wada, Y., & Yanagida, S. (1998). *Sol. Energy Mater. Sol. Cells*, 55, 113.
- [7] Lin, C. J., Yu, W. Y., & Chien, S. H. (2008). *Appl. Phys. Lett.*, 93, 133107.
- [8] Cahen, D., Hodes, G., Grätzel, M., Guillemoles, J. F., & Riess, I. (2000). *J. Phys. Chem. B*, 104, 2053.
- [9] Redmond, G., Fitzmaurice, D., & Grätzel, M. (1994). *Chem. Mater.*, 6, 686.
- [10] Rao, T. N., & Bahadur, L. (1997). *J. Electrochem. Soc.*, 144, 179.
- [11] Ai, X., Guo, J., Anderson, N. A., & Lian, T. (2004). *J. Phys. Chem. B*, 108, 12795.
- [12] Sayama, K., Sugihara, H., & Arakawa, H. (1998). *Chem. Mater.*, 10, 3825.
- [13] Lenzenmann, F., Krueger, J., Burnside, S., Brooks, K., Grätzel, M., Gal, D., Rühlle, S., & Cahen, D. (2001). *J. Phys. Chem. B*, 105, 6347.
- [14] Tan, B., Toman, E., Li, Y., & Wu, Y. (2007). *J. Am. Chem. Soc.*, 129, 4162.
- [15] Hardee, K. L., & Bard, A. J. (1976). *J. Electrochem. Soc.*, 123, 1024.
- [16] Tennakone, K., Kumara, G. R. R. A., Kottegoda, I. R. M., & Perera, V. P. S. (1999). *Chem. Commun.*, 15.
- [17] Kitiyanan, A., & Yoshikawa, S. (2005). *Mater. Lett.*, 59, 4038.
- [18] Kitiyanan, A., Kato, T., Suzuki, Y., & Yoshikawa, S. (2006). *J. Photochem. Photobiol. A*, 179, 130.
- [19] Palomares, E., Clifford, J. N., Haque, S. A., Lutz, T., & Durrant, J. R. (2003). *J. Am. Ceram. Soc.*, 125, 475.

- [20] Zaban, A., Chen, S. G., Chappel, S., & Gregg, B. A. (2000). *Chem. Commun.*, 2031.
- [21] Jung, H. S., Lee, J. K., Nastasi, M., Lee, S. W., Kim, J. Y., Park, J. S., Hong, K. S., & Shin, H. (2005). *Langmuir*, 21, 10332.
- [22] Cromer, D. T., & Herrington, K. (1955). *J. Am. Chem. Soc.*, 77, 4708.
- [23] Rostoker, W. (1952). *J. Met.*, 4, 981.